'Clicking' molecular hooks on silica nanoparticles to immobilize catalytically important metal complexes: the case of gold catalyst immobilization†

Anal Kr. Ganai,[a] Rima Bhardwaj,[b] Srinivas Hotha,*[b] Sayam Sen Gupta*[c] and B. L. V. Prasad*[a]

Received (in Montpellier, France) 19th April 2010, Accepted 24th June 2010
DOI: 10.1039/c0nj00292e

Gold mediated reactions have emerged as one of the best choices for affecting a variety of chemical transformations with a wide range of functional group tolerance. Application of such transformations to industrial processes necessitates immobilization of the Au ions into a matrix for easy separation of the catalyst after reaction. We report the synthesis and characterization of silica nanoparticles in which Au(III) has been immobilized through a 1,2,3-triazole linkage using an alkynalated picolinic acid exploiting "click chemistry". The Au(III) immobilized silica nanoparticle has been thoroughly characterized using FT-IR, ^{13}C CP MAS NMR and XPS. The utility of these particles as an easily separable catalyst for the Hashmi phenol synthesis is also reported.

Introduction

Homogeneous catalysts have been shown to catalyze various classes of organic reactions such as oxidation, reduction, C–C bond/C–heteroatom bond formation and polymerization.[1] High reaction rates and selectivity displayed by them have been attributed to their solubility and the accessibility of the catalytic sites to reactants in the reaction medium. Although tremendous progress has been made in the field of homogeneous catalysis during the last couple of decades, their application in industrial processes has been limited.[1] One of the reasons for this is the difficulty in separating the precious metal catalysts like Ir, Pt and Au from the product. Heterogeneous catalysts have been made by immobilization of homogeneous catalysts onto various insoluble supports to overcome this problem.[2] Although such a methodology allows easy separation of the metal catalyst, a substantial decrease in activity and selectivity of the immobilized catalysts is frequently observed due to the heterogeneous nature of these support materials in reaction media.[3–8]

In recent years, several efforts have been made to design dispersible matrices for catalyst immobilization.[9–11] This allows reactions to be performed under near homogeneous conditions and also allows catalyst separation after the reaction by methods like filtration or addition of another solvent. Such a methodology is very attractive since it combines the best of homogeneous and heterogeneous catalysis. Several such dispersible matrices have been explored. Nanoparticles have emerged as an alternative dispersible matrix for supporting homogeneous organic reactions.[12] They are considered semi-heterogeneous since they readily disperse in many solvents and the high surface area of these particles allows higher catalyst loading capacity than many conventional support matrices leading to improved catalytic activity. Some of these particles are even amenable to magnetic separation, thus making catalyst separation very easy. Among several nanoparticles that can be used as a support, the use of silica nanoparticles as a matrix for immobilization has been widespread.[13–15] This can be attributed to the advances made in the last decade or so regarding the development of methodologies that allows easy surface functionalization of silica nanoparticles.[16,17] Several organic groups can now be covalently attached to a silica nanoparticle surface using silanol chemistry. These organic functionalities can then be used to immobilize metal ions. Further, silica particles can also be synthesized with a magnetic core, thus, avoiding catalyst separation by filtration alone.

In the current decade, gold mediated reactions have emerged as one of the best choices for affecting a variety of chemical transformations with a wide range of functional group tolerance.[18–20] Several reactions have been developed with homogeneous Au catalysts and they have exploited the propensity of Au to activate carbon–carbon π-bonds as electrophiles.[18] Gold has come to be regarded as an exceedingly mild, relatively carbophilic Lewis acid, leading to the development of a broad array of reactions that proceed by the activation of unsaturated carbon–carbon bonds. Such C–C bond formation reactions are unique for Au which are otherwise very difficult to obtain from other transition metals. The excellent selectivity coupled with interesting possibilities for the synthesis of many novel molecular scaffolds hase invigorated interest among

[a] *Materials Chemistry Division, National Chemical Laboratory, Dr HomiBhabha Road, Pune 411008, India. E-mail: pl.bhagavatula@ncl.res.in; Fax: +91-20-25902636; Tel: +91-20-25902013*
[b] *Division of Organic Chemistry and National Chemical Laboratory, Dr HomiBhabha Road, Pune 411008, India. E-mail: s.hotha@ncl.res.in*
[c] *Chemical Engineering and Process Development Division, National Chemical Laboratory, Dr HomiBhabha Road, Pune 411008, India. E-mail: ss.sengupta@ncl.res.in*

† Electronic supplementary information (ESI) available: Spectra, linear isotherms and results of Hashmi reaction time course studies. See DOI: 10.1039/c0nj00292e

various scientific disciplines resulting in elegant strategies for easy synthesis of chemical architectures which are otherwise not possible or easy. The dynamic and exorbitant price of gold puts the chemistry of gold in an uncomfortable position though these reactions occur with catalytic quantities of gold. Thus, immobilization of gold could enable the use of gold catalysts with increased efficiency due to the increased local concentration of the Au. Corma *et al.* have immobilized Au(III) complexes onto MCM-41 and have used them as catalysts for Suzuki, Sonogoshira and Heck C–C bond formation reactions as well as hydroamination.[21–24] However, there are very few reports of heterogenized Au(III) complexes that activate carbon–carbon π-bonds as electrophiles. Nanoparticles of gold supported on nanocrystalline CeO_2 have been used to catalyze Hashmi's phenol synthesis – a reaction in which Au(III) activates a terminal alkyne to isomerize ω-alkynylfurans to phenols.[21] Further, initial leaching of Au was observed in the first run of the reaction. Thus, we envisioned that synthesis of Au(III) immobilized onto silica nanoparticles would yield a dispersible semi-heterogeneous system that might be very efficient in catalyzing unique organic transformations such as the thoroughly studied Hashmi phenol synthesis that has a wide variety of implications.

This study reports the synthesis and characterization of silica nanoparticles in which Au(III) has been immobilized through a 1,2,3-triazole linkage using an alkynalated picolinic acid exploiting "click chemistry" (Cu(I) catalyzed azide-alkyne cycloaddition reaction, CuAAC). Among the various surface functionalization techniques, CuAAC has become the most powerful "click chemistry" tool for conjugation between appropriately functionalized binding partners on surfaces *via* a 1,2,3-triazole linkage.[25,26] As a model study for the activation of carbon–carbon π-bonds as electrophiles, the catalytic activity of the Au(III) immobilized on silica nanoparticle was investigated for the Hashmi phenol synthesis The immobilized picolinic acid moiety on the silica surface has a dual role. It anchors the Au(III) and also increases the rate of the isomerization reaction as has been reported by Hashmi before.[27] The fate of Au(III) at the end of each run is also discussed.

Experimental

Materials

Ludox AS40 (50% by weight), 3-hydroxypicolinic acid, *o*-hydroxybenzoic acid, sodium tetrachloroaurate(III) dihydrate ($NaAuCl_4$), propargyl bromide, chloropropyltriethoxysilane (99%), *t*-butylammonium chloride, disodium bathophenanthroline sulfonate and copper iodide were obtained from Sigma Aldrich and used as received. Triethylamine was obtained from Spectrochem India. Sodium azide was obtained from Loba Chemie, India. All other chemicals and solvents were obtained from Merck, India and used as received. 3-Azidopropyltriethoxysilane (AzPTES), sodium dithiocarbamate and azide grafted silica nanoparticles (N_3-silica) were prepared as reported before.[28] Millipore water was used for the preparation and reactions of silica nanoparticles.

Synthesis

Prop-2-ynyl 3-(prop-2-ynyloxy)picolinate (1b). To an ice cooled suspension of 3-hydroxypicolinic acid **1a** (2.5 g, 0.018 mol) in 30 mL anhydrous *N*,*N*-dimethylformamide was added K_2CO_3 (11.7 g, 0.085 mol) at 0 °C. After 30 min, propargyl bromide (4.0 mL, 5.3 g, 0.045 mol) was added dropwise and stirred for 5 h at room temperature. At the end of the reaction (monitored by TLC), 40 mL water was added and extracted with diethyl ether (3 × 50 mL), the combined organic layers were washed with brine solution (2 × 20 mL), dried over anhydrous sodium sulfate and concentrated *in vacuo* to obtain a crude residue that was purified by silica gel column chromatography using ethyl acetate–petroleum ether (1 : 3 — b.p. 40–60 °C) to obtain the title compound **1b** (3.4 g, 89%) as a gum. (Scheme 1)

^{1}H NMR (200.13 MHz, $CDCl_3$): δ 2.54 (t, 1H, J = 2.5 Hz), 2.60 (t, 1H, J = 2.4 Hz), 4.84 (d, 2H, J = 2.4 Hz), 4.98 (d, 2H, J = 2.5 Hz), 7.46 (dd, 1H, J = 4.4, 8.6 Hz), 7.57 (dd, 1H, J = 1.3, 8.6 Hz), 8.36 (dd, 1H, J = 1.1, 4.4 Hz); ^{13}C NMR (50.32 MHz, $CDCl_3$): δ 52.8, 56.7, 75.3, 77.1, 77.1, 77.2, 122.4, 127.1, 138.5, 142.0, 153.7, 163.5. For the ^{1}H and ^{13}C NMR spectra see ESI-1†; M_w Calcd for $C_{12}H_9NO_3Na$: 238.204; Found, 238.162.

Prop-2-ynyl 3-(prop-2-ynyloxy)picolinic acid (L1). LiOH (223 mg, 9.3 mmol) in water (5 mL) was added to a solution of compound **1b** (1.0 g, 4.65 mmol) in 15 mL of CH_3OH–THF (1 : 2) at 0 °C. The reaction mixture was stirred at room temperature until the starting material was completely consumed (TLC) and then the solution was neutralized using amberlite IR120 (H^+), filtered, and the resin was washed with water and MeOH. The combined methanolic solution was concentrated under reduced pressure and the crude product (0.9 g) was recrystallized from aqueous ethanol to give compound **L1** (0.6 g, 73%) as a solid.

m.p. 63 °C; ^{1}H NMR (200.13 MHz, $CDCl_3$): δ 2.75 (t, 1 H, J = 2.4 Hz), 4.06 (d, 2 H, J = 2.4 Hz), 6.67 (dd, 1 H, J = 4.5, 8.6 Hz), 6.80 (dd, 1 H, J = 1.2, 8.6 Hz), 7.34 (dd, 1 H, J = 1.2, 4.5 Hz); ^{13}C NMR (50.32 MHz, $CDCl_3$): δ 56.5, 78.9, 79.6, 122.3, 126.7, 141.7, 142.1, 151.6, 167.0. For the ^{1}H and ^{13}C NMR spectra see ESI-2†; M_w Calcd for $C_9H_7NO_3$: 177.157; Found, 178.214 (M^+ + 1).

Prop-2-ynyl 2-(prop-2-ynyloxy)benzoate (2b). This has been synthesized from compound **2a** according to the procedure similar to that one used for **1b**.

m.p. 167 °C; ^{1}H NMR (see ESI-2†) (200.13 MHz, $CDCl_3$): δ 2.52 (t, 1 H, J = 2.5 Hz), 2.55 (t, 1 H, J = 2.4 Hz), 4.80 (d, 2 H, J = 2.4 Hz), 4.89 (d, 2 H, J = 2.5 Hz), 7.04 (t, 1 H, J = 7.5 Hz), 7.13 (d, 1 H, J = 8.5 Hz), 7.49 (t, 1 H, J = 7.7 Hz), 7.86 (dd, 1 H, J = 1.6, 7.7 Hz); ^{13}C NMR (50.32 MHz, $CDCl_3$): δ 52.3, 56.8, 74.9, 76.1, 77.8, 78.1, 114.4, 119.9, 121.3, 132.0,

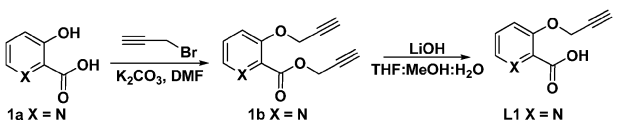

Scheme 1 Synthesis of ligand **L1** and ligand **L2**.

133.8, 157.3, 164.8. For the ^{1}H and ^{13}C NMR spectra see ESI-3†; LRMS Calcd for $C_{13}H_{10}O_3Na$: 237.217; Found, 237.062.

Prop-2-ynyl 2-(prop-2-ynyloxy)benzoic acid (L2). It has been prepared by following the above procedure (for **L1**) from compound **2b**.

m.p. 65 °C; ^{1}H NMR (200.13 MHz, $CDCl_3$): δ 2.51 (m, 1 H), 3.60 (t, 1 H, J = 2.41 Hz), 4.87 (d, 2 H, J = 2.4 Hz), 7.04 (dt, 1 H, J = 0.9, 7.5, 14.2 Hz), 7.19 (d, 1 H, J = 8.7 Hz), 7.51 (m, 1 H), 7.65 (dd, 1 H, J = 1.8, 7.7 Hz); ^{13}C NMR (50.32 MHz, $CDCl_3$): δ 56.6, 76.3, 77.5, 121.5, 123.7, 138.2, 142.7, 153.6. For the ^{1}H and ^{13}C NMR spectra see ESI-4†; M_w Calcd for $C_{10}H_8O_3$:176.169. Found, 177.108

Ligand (L1 or L2) functionalized silica nanoparticles using CuAAC. For CuAAC, the azide functionalized silica nanoparticles were incubated with 5 equivalents of the alkyne substituted ligand (**L1** or **L2**) in a DMF–H_2O solvent mixture (8 : 2) containing CuI (2.0 equivalents), disodium bathophenanthrolene sulfonate (2.0 equivalents), sodium ascorbate (4 equivalents) and triethylamine (5.0 equivalents). In a typical reaction, azide grafted silica nanoparticles (150 mg, 0.1071 mmol of azide) were incubated with **L1** (94.78 mg, 0.5355 mmol, 5 eq.) in a 12 ml DMF + 3 ml H_2O mixture containing sodium ascorbate (84.82 mg, 0.4284 mmol, 4 eq.) and copper iodide (40.698 mg, 0.2142 mmol, 2 eq.) and disodium sulfonated bathophenanthroline (115.56 mg, 0.2142 mmol, 2 eq.) and triethylamine (54 mg, 0.5355 mmol, 5 eq.). The reaction mixture was subjected to three freeze–pump–thaw cycles for rigorous exclusion of dioxygen. The CuAAC was allowed to proceed for 24 h with stirring. After completion of the reaction, the mixture was taken into a centrifuge tube and centrifuged for 20 min at 12 000 rpm. The supernatant liquid was decanted off and the solid residue was washed with DMF (2 times), ethanol (2 times), 0.1 M sodium ascorbate (2 times), 0.1 M *N*,*N*-diethyldithiocarbamate sodium in ethanol (4 times) and ethanol (2 times). It was finally washed with 0.1 M HCl (2 times) and then stored as a suspension in ethanol. This sample will henceforth be called silica-**L1**. For preparation of samples for NMR and IR, a part of the functionalized silica nanoparticles solution was washed in ethanol and dried under vacuum at 60 °C. Yield: 123 mg

A similar protocol was adopted for CuAAC of the ligand **L2** with silica-azide to afford the conjugate silica-**L2**. Yield: 112 mg

Silica-Au-L1. Functionalized silica nanoparticles silica-**L1** were dispersed in methanol and then $NaAuCl_4$ was added and heated at 60 °C. In a typical reaction, 50 mg of silica-**L1** (0.03882 mmol) were dispersed in 2.5 ml methanol followed by the addition of 16.85 mg $NaAuCl_4$ (0.0465 mmol, 1.2 eq.). The reaction mixture was heated to 60 °C for 10 h. After completion of the reaction, the mixture was taken into a centrifuge tube and centrifuged for 10 min at 12 000 rpm. The supernatant liquid was decanted off and the solid residue was washed with methanol (5 times) to afford silica-**Au-L1**. It was finally stored as a suspension in ethanol. For preparation of samples for IR, a part of the silica-**Au-L1** solution was washed in ethanol and dried under vacuum at 60 °C. Yield: 41 mg (Scheme 2).

4-Methyl-1,3-dihydroisobenzofuran-5-ol (4). $AuCl_3$ (4 mg, 0.013 mmol) in acetonitrile (0.5 mL) was added to a solution of 2-methyl-5-(prop-2-ynyloxy)methyl furan **3** (100 mg, 0.67 mmol) in acetonitrile (1 mL) at 0 °C. The reaction mixture was stirred at room temperature until the starting material was completely consumed and then quenched with Et_3N and concentrated in *vacuo*. The crude residue was purified by silica gel column chromatography using ethyl acetate–petroleum ether (1 : 20) to obtain the title product **4** (90 mg, 90%).

m.p. 71 °C; ^{1}H NMR (200.13 MHz, $CDCl_3$): δ 2.25 (s, 3 H), 5.13 (brs, 2 H), 5.14 (brs, 2 H), 5.77 (s, 1 H), 6.70 (d, 1 H, J = 7.5 Hz), 7.04 (d, 1 H, J = 7.5 Hz); ^{13}C NMR (50.32 MHz, $CDCl_3$): δ 15.2, 71.7, 74.0, 112.7, 122.2, 124.9, 130.5, 138.6, 148.4. For the ^{1}H and ^{13}C NMR spectra see ESI-5†; M_w Calcd for $C_9H_{10}O_3$:150.174; Found, 150.938.

General procedure of the Hashmi reaction for the synthesis of 4-methyl-1,3-dihydroisobenzofuran-5-ol using silica-Au-L1. Silica-Au-**L1** (2 mol% Au, 28.2 mg, 0.01027 mmol) in acetonitrile (1 mL) was added to a solution of 2-methyl-5-(prop-2-ynyloxy)methyl furan (**3**) (75 mg, 0.5136 mmol) in acetonitrile (0.5 mL) at 0 °C. The reaction mixture was stirred at room temperature and periodically monitored by LC-MS until the starting material was completely consumed. After the consumption of the starting material, the catalyst was separated by centrifuging at 6000 rpm and then washed with acetonitrile, sonicated and dried for 30 min. The recovered catalyst was reused for one more cycle of the same reaction.

5-Methyl-2-tosylisoindolin-4-ol (6). Reaction was carried out for 5 h with substrate **5**. The reaction conditions were kept similar to those followed in the reaction of **3** to give **4** as delineated above (Scheme 3). m.p. 178 °C; ^{1}H NMR (200.13 MHz, $CDCl_3$): δ 2.19 (s, 3 H), 2.40 (s, 3 H), 4.60 (m, 4 H), 5.00 (brs, 1 H), 6.64 (d, 1 H, J = 7.6 Hz), 6.99 (d, 1 H, J = 7.5 Hz), 7.30 (d, 2 H, J = 8.0 Hz), 7.75 (d, 2 H, J = 8.4 Hz); ^{13}C NMR (100.61 MHz, $CDCl_3$): δ 15.1, 21.5, 51.6, 54.0, 114.4, 120.1, 122.5, 127.6 (2C), 129.8 (2C), 130.7, 135.5, 135.8, 143.7, 149.0; For the ^{1}H and ^{13}C NMR spectra see ESI-6†; M_w Calcd for $C_{16}H_{17}NO_3S$: 303.092; Found, 304.291 (M^+ + 1).

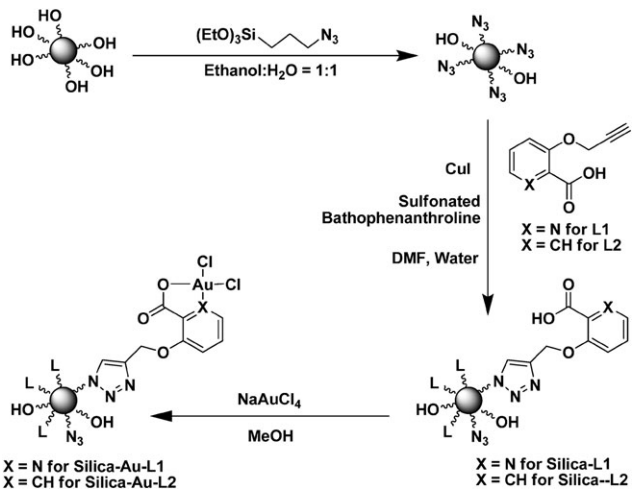

Scheme 2 Synthesis of silica-Au-**L1** conjugate.

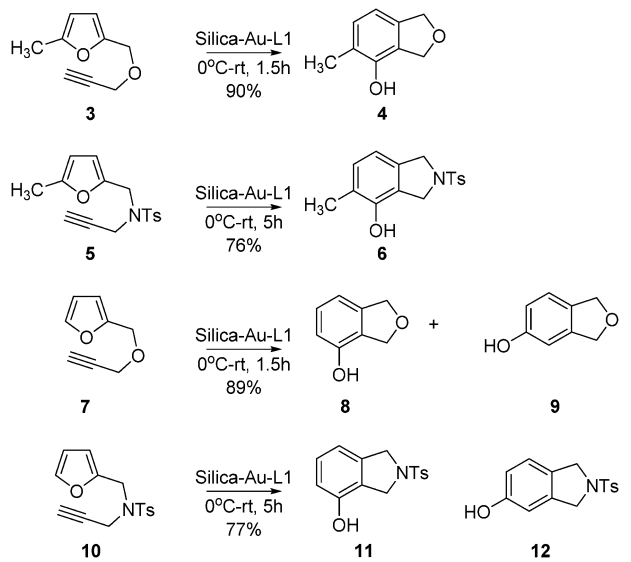

Scheme 3 Experimental details of the Hashmi reaction performed using silica-Au-**L1** conjugate on various substrates.

When the reaction was carried out with substrate **7** two products **8** and **9** were obtained. The reaction conditions were again kept the same as those delineated above (Scheme 3).

Dihydroisobenzofuran-4-ol (8). m.p. 130–135 °C; ^{1}H NMR (400.13 MHz, $CDCl_3$): δ 5.13, 5.15 (2s, 4 H), 5.67 (brs, 1 H), 6.66 (d, 1 H, J = 8.1 Hz), 6.81 (d, 1 H, J = 7.6 Hz), 7.15 (t, 1 H, J = 7.8 Hz); ^{13}C NMR (100.61 MHz, $CDCl_3$): δ 71.4, 73.7, 112.8, 113.4, 124.9, 128.8, 141.2, 149.9. For the ^{1}H and ^{13}C NMR spectra see ESI-7†; M_w Calcd for $C_8H_8O_2$: 136.052; Found, 137.114 (M^+ + 1).

1,3-Dihydroisobenzofuran-5-ol (9). m.p. 120 °C; ^{1}H NMR (200.13 MHz, $CDCl_3$): δ 5.06 (s, 4 H), 5.50 (brs, 1 H), 6.66–6.78 (m, 2 H), 7.08 (d, 1 H, J = 8.0 Hz); ^{13}C NMR (50.32 MHz, $CDCl_3$): δ 73.3, 73.4, 107.9, 114.6, 121.8, 130.7, 140.7, 155.5. For the ^{1}H and ^{13}C NMR spectra see ESI-8†; M_w Calcd for $C_8H_8O_2$: 136.052; Found, 137.020 (M^+ + 1).

When the reaction was carried out with substrate **10** two products **11** and **12** were obtained. The reaction conditions were again kept the same as those delineated above (Scheme 3).

2-Tosylisoindolin-4-ol (11). m.p. 145–150 °C; ^{1}H NMR (200.13 MHz, $CDCl_3$): δ 2.40 (s, 3 H), 4.53 (s, 4 H), 5.27 (s, 1 H), 6.68 (td, 2 H, J = 2.4, 8.2 Hz), 7.00 (d, 1 H, J = 8.2 Hz), 7.31 (m, 2 H), 7.75 (m, 2 H); ^{13}C NMR (100.61 MHz, $CDCl_3$): δ 21.5, 53.2, 53.7, 109.5, 115.2, 123.6, 127.6(2C), 127.9, 129.9(2C), 133.6, 137.7, 143.8, 155.6. For the ^{1}H and ^{13}C NMR spectra see ESI-9†; M_w Calcd for $C_{15}H_{15}NO_3S$: 289.077; Found, 290.203 (M^+ + 1).

2-Tosylisoindolin-5-ol (12). m.p. 170 °C; ^{1}H NMR (200.13 MHz, $CDCl_3$): δ 2.40 (s, 3 H), 4.67 (s, 4 H), 5.52 (brs, 1 H), 6.64 (d, 1 H, J = 8.1 Hz), 6.72 (d, 1 H, J = 7.6 Hz), 7.10 (t, 1 H, J = 7.9 Hz), 7.31 (m, 2 H), 7.77 (m, 2 H); ^{13}C NMR (50.32 MHz, $CDCl_3$): δ 21.6, 51.6, 54.1, 114.1, 114.7, 122.8, 127.6 (2C), 129.4, 129.9 (2C), 133.6, 138.3, 143.8, 150.9. For the ^{1}H and ^{13}C NMR spectra see ESI-10†; M_w Calcd for $C_{15}H_{15}NO_3S$: 289.077; Found, 290.276 (M^+ + 1).

Characterization

HR-TEM images were taken on a FEI Technai F30 operating at 300 kV. The samples were prepared by dispersing 0.1 mg of nanoparticles in 1 mL of ethanol by sonication, and drop casting 3 μL of the resulting suspension on a carbon coated copper grid of 400 mesh and allowed to dry in air. FT-IR spectra were recorded on a Perkin Elmer FT-IR spectrum GX instrument by making KBr pellets. Pellets were prepared by mixing 3 mg of sample with 97 mg of KBr. Elemental analyses were carried out on a Thermo Finnigan FLASH EA 1112 series instrument.

^{29}Si and ^{13}C Cross Polarization Magic Angle Spinning (CPMAS) NMR experiments were carried out on a Bruker AVANCE 300 wide bore spectrometer equipped with a superconducting magnet with a field of 7.1 Tesla. The operating frequencies for ^{13}C and ^{29}Si were 300 MHz, 75.4 MHz and 59.6 MHz, respectively. The samples were packed into a 4 mm zirconia rotor and loaded into a 4 mm BL MAS probe and spun about the magic angle (54.74) at 10 KHz using a standard ramp-CP pulse sequence was used for both the experiments. The RF-powers were 50 kHz and 60 kHz for the ^{29}Si and ^{13}C CPMAS experiments. The contact times were 6 ms and 3 ms for the ^{29}Si and the ^{13}C CPMAS experiments. All the chemical shifts were referenced to TMS. Typically 10 000 to 25 000 scans with a recycle delay of 3 s were collected depending on the sensitivity of the sample.

Thermogravimetric analysis (TGA) of the silica nanoparticles was carried out using a TA Instrument SDT Q600 analyzer between 20 and 800 °C in air (flow 50 ml min^{-1}) at a heating rate of 10 °C min^{-1}. All samples were dried under vacuum at 60 °C overnight prior to TGA runs. The graft density of the grafted moiety on the silica surface was determined by thermogravimetric analysis (TGA) using the following equation as described before.[29]

$$\text{Graft density } (\mu\text{mol m}^{-2}) = \frac{\frac{W_{\text{silica}(60-600)}}{100-W_{\text{silica}(60-600)}} \times 100 - W_{\text{Ludox}(60-600)}}{M \times S \times 100} \times 10^6$$

Where W_{60-600} is the weight loss between 60 and 600 °C corresponding to the decomposition of the grafted silica molecule corrected from the thermal degradation and M is the molecular weight of the grafted silane. S represents the specific surface area of the silica nanoparticle (measured as 110 m^2 g^{-1}) while W_{Ludox} represents the determined weight loss of silica before grafting.

For XPS analysis the gold coordinated functionalized silica nanoparticles were deposited on a sample holder by spreading the powder. The measurements were carried out on a VG MicroTech ESCA 3000 instrument at a pressure of better than 10^{-9} Torr. The general scan and Si 2p, C 1s, N 1s, O 1s, Cl 2p and Au 4f core level spectra were recorded with unmonochromatized Mg-Kα radiation (photon energy ~1253.6 eV) at pass energy of 50 eV and electron take off angle (angle between electron emission direction and surface

plane) of 60°. The overall resolution of measurement is thus 1 eV for the XPS measurements. The core level spectra were background corrected using the Shirley algorithm.[30] The core level binding energies (BE) were aligned with the silica binding energy of 103.4 eV.

ICP experiments were performed on a Thermo IRIS Intrepid spectrum apparatus. The typical procedure used is as follows: the calculated amount of sample was dried *in vacuo* overnight was taken into a beaker and heated with aqua-regia for 20 min. It was then filtered and volume was made up to 24 mL with aqua-regia in a volumetric flask. This stock solution was then diluted using millipore water and was analyzed by using the ICP instrument for quantitative determination of Au.

Nitrogen adsorption and desorption studies at −196 °C were carried out using an Quadrasorb SI instrument. Before the nitrogen adsorption measurements, the samples were degassed overnight under vacuum using a FloVac Degasser at 300 °C (for silica) or at 100 °C (for modified silicas). Multipoint BET surface area was obtained from the nitrogen adsorption isotherm in the relative pressure range from 0.15 to 0.5.

Results and discussion

Our strategy to prepare the desired "molecular hook" for immobilizing a gold(III) complex onto silica is displayed in Scheme 2. The first step in this endeavour was the synthesis of azide grafted silica particles.

Synthesis of azide grafted silica nanoparticles

The azide grafted silica nanoparticles (N_3-silica) were synthesized by the condensation of azidopropyltriethoxysilane (AzPTES) onto a commercially available silica colloidal solution (Ludox AS40; 22 ± 3 nm particle size; nonporous spherical material of surface area 110 $m^2\ g^{-1}$; see ESI-11†). Elemental and thermogravimetric analyses confirmed a grafting ratio of 0.7 mmol of azidopropyl group per gram of silica particle (Fig. 1a and b). The nitrogen content was found to be 3.4% while the TGA data displayed a loss of 7.2% in weight. Taking into consideration that the average particle size is 22 nm and a surface area of 110 $m^2\ g^{-1}$, the grafting density was determined to be 3.7 azidopropyl groups per nm^2. It has been calculated that 3–5 silanol sites per nm^2 are available for condensation of organosilane molecules on the silica surface for monolayer coverage.[16] Therefore, the grafting density of 3.7 azidopropyl groups per nm^2 signifies monolayer coverage of the azidopropyl

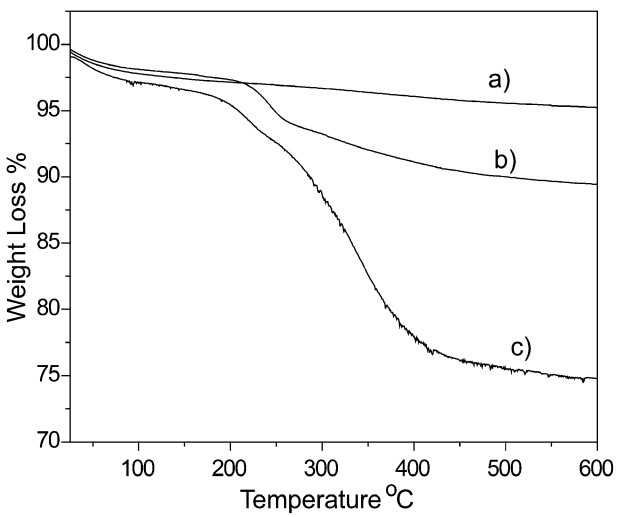

Fig. 1 Thermogravimetric analysis (TGA) of (a) bare Ludox, (b) N_3-silica, (c) silica-**L1**.

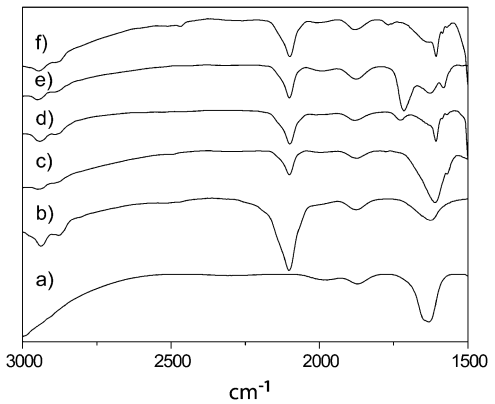

Fig. 2 Infrared spectra of (a) bare Ludox, (b) N_3-silica, (c) silica-**L1**, (d) silica-**L2**, (e) silica-**Au-L1**, and (f) silica-**Au-L2**.

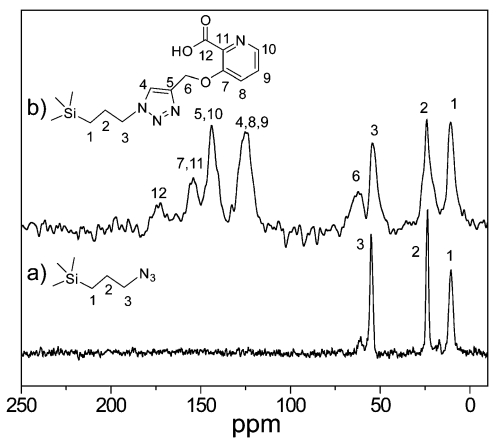

Fig. 3 ^{13}C CP-MAS NMR of (a) N_3-silica and (b) silica-**L1**.

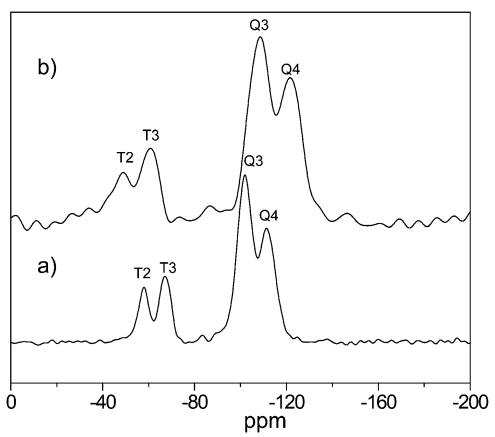

Fig. 4 ^{29}Si CP-MAS NMR of (a) N_3-silica and (b) silica-**L1**.

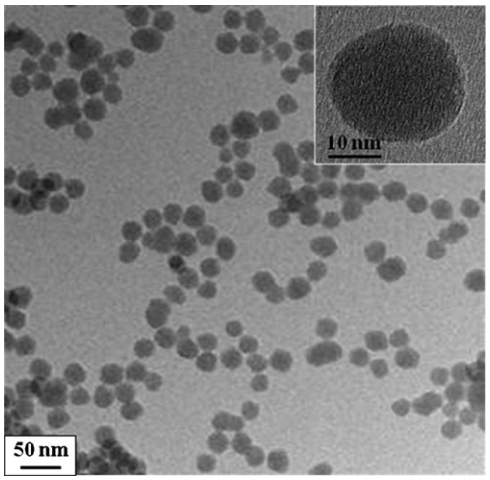

Fig. 5 TEM of N_3-silica.

groups on the silica surface. The azide grafted silica nanoparticles were characterized by FT-IR (Fig. 2b), multinuclear (^{13}C, ^{29}Si) solid state NMR (Fig. 3a and 4a) and TEM (Fig. 5) studies. In the FT-IR spectrum, appearance of the absorbance at $\sim$2100 cm^{-1} (which is absent in the starting Ludox particle) that is characteristic for the stretching vibration of organic azide (Fig. 2a and b) was observed. The solid state ^{13}C CP-MAS NMR spectrum of the azide grafted silica particles shows three peaks corresponding to C1 (10.81 ppm), C2 (23.66 ppm), C3 (54.95 ppm) that can be assigned to the three C-atoms of the azido-propyl chain (Fig. 3a). The ^{29}Si CP MAS NMR spectra of N_3-silica exhibit prominent peaks at around -111, -101, -67 and -58 ppm (Fig. 4a). The peaks at -111 and -101 ppm are assigned to the different types of the Si-sites namely Q3 [$(SiO)_3Si(OH)$] and Q4 [$(SiO)_4Si$]. Two other distinct peaks observed at -58 and -67 ppm are ascribed to the functionalized sites of the Si-framework namely T2 [$R(SiO)_2Si(OH)$] and T3 [$R(SiO)_3Si$], respectively, where R is the azidopropyl group. Thus, all these data conclusively prove that the azidopropyl group was grafted successfully onto the silica nanoparticle.

Synthesis and characterization of silica-L1 and silica-L2

The second step in our strategy was to modify the silica surface to bear the moieties **L1** or **L2** that would serve as hooks/anchors to immobilize Au(III). The ligand **L1** was chosen such that a robust five-membered ring would form once the Au(III) ligates. The CuAAC reaction was carried out using CuI/sulfonated bathophenanthroline in a DMF and H_2O mixture at a ratio of 80 : 20 for 24 h (Scheme 2). The extent of the reaction was estimated using IR spectroscopy by monitoring the decrease in the integrated intensity of the $\nu_{as}(N_3)$ at 2100 cm^{-1} (Fig. 2). Control reactions performed in the absence of CuI showed no conversion of the azide. After the reaction, an extensive washing protocol was followed to remove the Cu(I), ligand, ascorbate and any unreacted **L1**. The attachment of **L1** was further confirmed by the appearance of the ν(C=O) at 1610 cm^{-1} arising from the carboxylic moiety present in **L1**. The amount of grafted **L1** in silica-**L1** was determined to be 0.53 mmol per g of silica by semi-quantitative IR.[28] This corresponds to a conversion of 75% of the available azides to the corresponding triazoles. Moreover, the TG-DTA analysis of silica-**L1** (Fig. 1c) indicated a mass loss of 20% between 200 °C and 600 °C which corresponds to a loading of 0.65 mmol of **L1** per g of silica (see Table 1). The graft density was estimated to be about 3.6 groups per nm^2 (6 μmol m^{-2}). The grafting density of silica-**L1** obtained by FT-IR was slightly lower than that estimated by TG-DTA. This could be due to the fact that the increase in the molar mass of the nanoparticles due to the addition of **L1** was not considered during the estimation of the extent of reaction. For control experiments, ligand **L2** was grafted onto the silica nanoparticles using a similar methodology to that described above. It should be noted that **L2** has only one carboxylate ligand and hence is not expected to bind Au(III). The grafting density of **L2** in silica-**L2** was determined to be 0.59 mmol per g of silica which corresponds to the conversion of 85% of the available azides to the corresponding triazoles. The presence of Cu in silica-**L1** and silica-**L2** was tested using ICP. No appreciable amount of Cu was found which indicates that the extensive washing protocol used was sufficient to remove all of the Cu from these hybrid materials.

Table 1 The calculated ligand grafting density and gold loading on different functionalized silica particles

	Weight loss (%)	Ligand grafting density (mmol g^{-1})	[Au] (mmol g^{-1})
Ludox	2	—	—
N_3-silica	7.2	0.684	0.005
Silica-L1	19.62	0.65	—
Silica-Au-L1	—	0.65	0.339
Silica-L2	—	0.59	—
Silica-Au-L2	—	—	0.09

The solid state ^{13}C CP-MAS NMR spectra of silica-**L1** displayed extra peaks in addition to the C1, C2 and C3 observed in N_3-silica (Fig. 3b). The extra resonances at 128 ppm and 144 ppm correspond to the C4 and C5 atoms of the triazole indicating a covalent linkage of **L1** *via* the triazole ring. The C7 peak observed at 183 ppm is due to the presence of the C=O group of the carboxylic acid. The ^{29}Si CP MAS spectrum of silica-**L1** showed little or no change from the starting azide grafted silica particles indicating that the Si-sites do not undergo any chemical change during the reaction and its work-up (Fig. 4b). This is expected since the T1 and T2 Si-sites are that from the azido-propyl modified silica and should not undergo any change during the course of the click reaction.

The chemical composition of silica-**L1** was also verified using X-ray photoelectron spectroscopy. All the pristine spectra have been background corrected using the Shirley algorithm[30] and the curves deconvoluted using standard curve fitting programs. The signals from the Si 1s core level could be resolved into three components mainly occurring at 102.0, 103.4, and 105.1 eV (Fig. 6A). These are assigned to Si–O–H, Si–O–Si, and Si–O–C, respectively. Three chemically distinct components are observed at 284.3, 285.7 and 287.9 eV in the case of the C 1s core level spectrum (Fig. 6B). The peak at $\sim$284 eV was ascribed to the adventitious carbon. The peak at higher binding energy at $\sim$286 eV could be ascribed

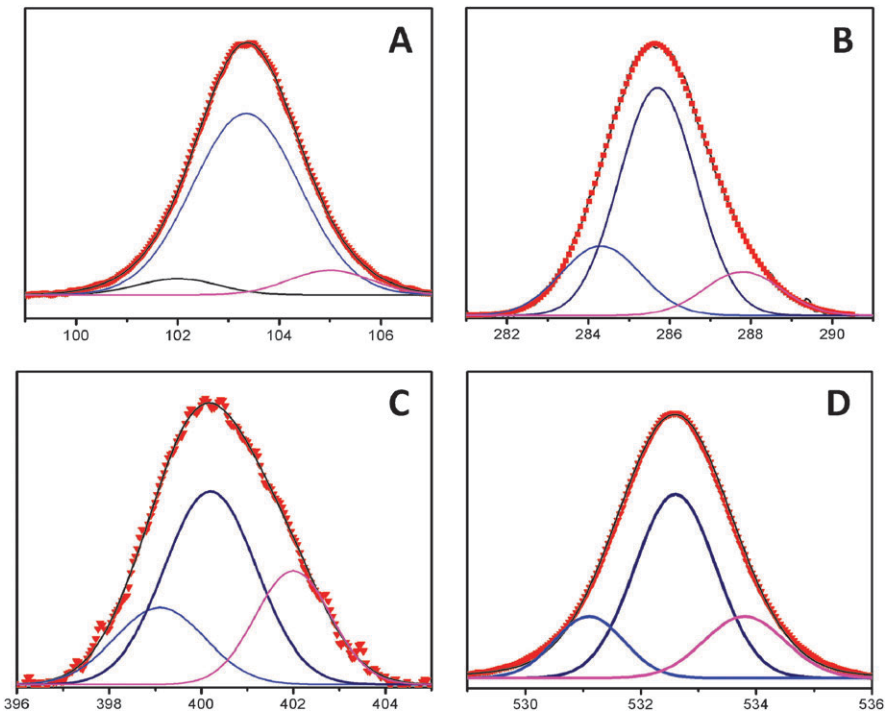

Fig. 6 XPS of silica-**L1**, (A) Si 2p, (B) C 1s, (C) N 1s, (D) O 1s core levels of silica-**L1**

to the carbon bound to N. On the other hand the peak at ~288 eV could be ascribed to the –C=O carbon. The O 1s signals can be deconvoluted to three components at 531.1, 532.6, and 533.8 eV which proves the presence of different components of O 1s (Fig. 6D). The high BE component at 533.8 eV is accredited to the loading of **L1** onto silica azide. Two chemically distinct components are observed at 399.1, 400.2 and 402.0 eV in the case of the N 1s core level spectrum (Fig. 6C). The higher binding energy was assigned to the pyridine N present in the **L1** molecule attached to silica.

Synthesis and characterization of Au(III) incorporated silica-L1

After thorough optimization, Au(III) was incorporated into silica-**L1** nanoparticle by incubating them with $NaAuCl_4$ in a methanol solution at 55 °C to afford silica-Au-**L1** (Scheme 2). The IR spectra of silica-Au-**L1** showed that the γ(CO) shifted significantly from 1610 cm^{-1} to 1720 cm^{-1}, suggesting the binding of Au(III) to the O-atom of the carboxylic acid of **L1**. Such shifts have been reported before for related Au(III) complexes with carboxylic containing ligands.[31,32] From the ICP analysis, Au concentration was determined to be 0.34 mmol per g of Silica-**L1**. This corresponds to the fact that Au(III) was bound to 55% of the available binding sites of the picolinic acid moiety of silica-**L1**.

The chemical composition of silica-Au-**L1** was also probed using X-ray photoelectron spectroscopy. The spectra have been background corrected using the Shirley algorithm prior to curve resolution. The signals from the Si 2p, C 1s, O 1s and N 1s were more or less similar to the earlier peaks observed for the starting silica-**L1**. Further, the Au 4f core level signals could be resolved into two chemically distinct species corresponding to Au(I) and Au(III) (Fig. 7A). The pair at 84.6 and 88.2 eV can be assigned as the spin orbit coupling of Au $4f_{7/2}$ and Au $4f_{5/2}$, respectively, of Au(I). The presence of signals at 85.5 eV and 89.1 eV is related to the presence of Au(III). It can be clearly seen that the Au(III) component is less when compared to Au(I), which is unusual. To probe this further, we prepared the complex bis(pyridine-2-carboxylato)-gold(III) perchlorate and recorded its XPS.[31] Interestingly, here also we could see peaks corresponding to Au(III) and Au(I), which is similar to the XPS of silica-Au-**L1** (Fig. 7D). The ambiguous detection of Au(I) can be attributed to the electron donating capability of **L1** to Au(III) and strong X-ray radiation while recording XPS.[33] However, we would like to mention that this did not influence in anyway the catalytic nature of the complex as can be seen further. The presence of chloride was confirmed from the peak at 198.8 eV (Fig. 7B).

Similar attempts were made to incorporate Au(III) onto silica-**L2**. However, the FT-IR of the resultant compound (silica-Au-**L2**) displayed no shift in the γ(CO) stretch as observed in silica-Au-**L1**. The Au concentration determined by ICP was found out to be only 0.09 mmol per g of silica-Au-**L2**. This was expected since the ligand **L2** does not have the bidentate picolinic acid moiety present as in **L1** that was necessary to bind the Au(III). The small amount of Au(III) seen from ICP was probably due to some non-specific binding to the surface silanol groups.

Hashmi phenol synthesis by Au immobilized silica nanoparticles

The catalysts silica-Au-**L1** and silica-Au-**L2** were then evaluated for their ability to activate the alkyne moiety of furanyl propargyl ether (**4**) to trigger an intramolecular Diels–Alder reaction to give isobenzofuran **5** (Scheme 3). Accordingly, 5-methylfuranyl propargyl ether (**4**) was treated with

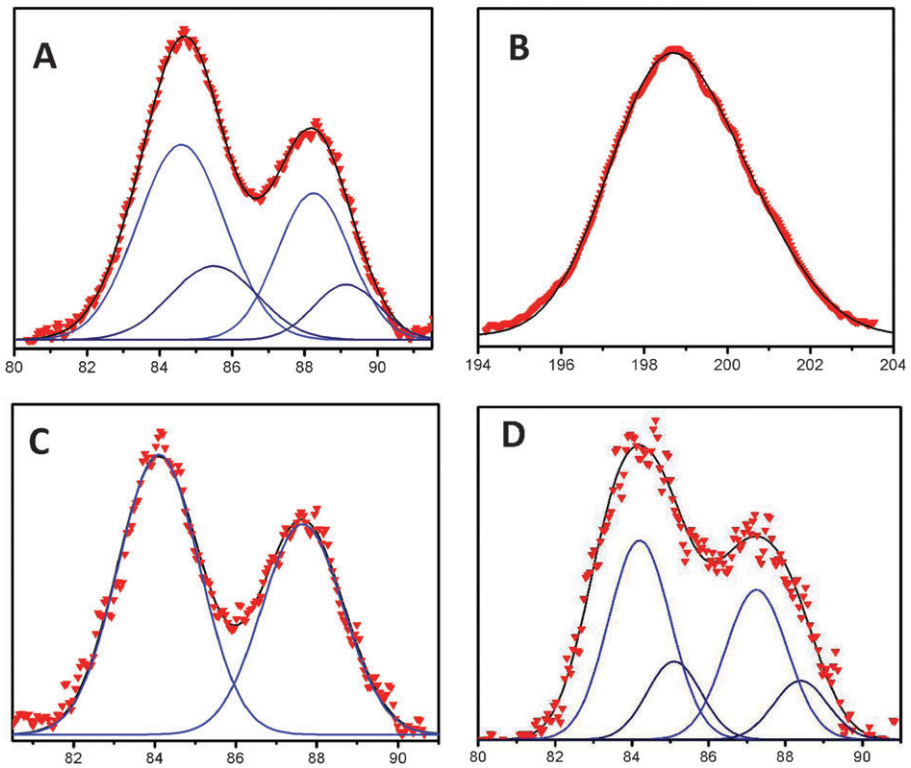

Fig. 7 XPS of (A) Au 4f of silica-Au-**L1**, (B) Cl 2p of silica-Au-**L1**, (C) Au 4f of the spent catalyst after 2nd run, (D) Au 4f of the complex bis(pyridine-2-carboxylato)-gold(III) perchlorate.

silica-Au-**L1** (2 mol% Au) in acetonitrile leading to the formation of the isobenzofuran (**5**). The reaction was found to be very exothermic and hence it was carried out at 0 °C. The reaction was complete in about 100 min as was observed from the complete disappearance of the starting material by LC-MS analysis (see ESI-12†). Isolation of the product showed the yield of the reaction to be 90%. The same reaction, carried out using $AuCl_3$ as the catalyst, took more than 3 h to undergo completion clearly exemplifying the advantages of silica-Au-**L1** over $AuCl_3$. This is expected since the picolinic acid ligand that binds the Au(III) in silica-Au-**L1** is known to accelerate the rate of the reaction, as has been shown by Hashmi *et al.*[27] In the control experiment, formation of isobenzofuran was not observed using silica-Au-**L2**. The catalyst silica-Au-**L2** does not contain appreciable amounts of Au(III) since **L2**, a monodentate ligand having only a carboxylic acid moiety, is unable to bind Au(III) effectively. This also clearly shows that the presence of Au(III) in silica-Au-**L1** is key to the progress of this reaction. At the end of the reaction, the silica-Au-**L1** could be isolated from the reaction mixture by centrifugation. Isolated silica-Au-**L1** particles were washed three times with acetonitrile, sonicated and then resuspended in acetonitrile to perform the Hashmi reaction on compound **4** again. This isolated catalyst was again found to be active for the synthesis of isobenzofuran **5** albeit taking longer periods of time for completion (16 h) (see ESI-13†). Subsequently, this catalyst was not found to be active for the synthesis of isobenzofurans. Therefore it was obvious that the catalyst was losing activity during the progress of the reaction. One possibility for this deactivation might be the leaching of Au during the progress of the reaction. The amount of Au present in silica-Au-**L1** was estimated after each catalytic cycle by ICP. It was determined that the amount of gold even after three cycles of reaction was within 15% of the initial loading. This negates the possibility of Au leaching as the reaction progresses. The XPS of the spent catalysts (Fig. 7C) after the second cycle of reaction displayed the spin orbit pair at 84.1 and 87.7 eV that can be assigned to Au(0). The presence of Au(0) indicates that during the progress of the reaction, the Au(III) complex was getting reduced to Au(0) thereby slowly rendering the catalyst inactive. As mentioned earlier, the reaction is very exothermic, and the heat generated during the reaction may have reduced Au(III) to Au(0) which corroborates the recent findings by Shi and co-workers.[34]

Similar reaction with silica-Au-**L1** was successfully carried out on compound **5** to obtain the phenol **6** in 76% yield though the reaction took 5 h whereas the control reaction with silica-Au-**L2** did not yield any product formation. Furthermore, we checked the efficacy of the silica-Au-**L1** with two other substrates **7** and **10** to obtain **8**, **9** and **11**, **12** in good yields (Scheme 3).

Conclusion

In conclusion, a successful strategy to immobilize Au(III) onto silica nanoparticles through a CuAAC "click chemistry" protocol has been demonstrated. The catalyst has been thoroughly and extensively characterized using a variety of analytical and spectroscopic techniques. The catalyst was found to activate the carbon–carbon π-bond of the alkynyl

group in Hashmi phenol synthesis. The same catalyst is being evaluated for other Au(III) catalyzed cascade reactions initiated by heteroatom nucleophiles with π-electrophiles. The developed methodology is a generic one and can be extended to immobilizing other metal complexes and/or other surfaces including magnetic core–shell systems. Studies in this direction are currently underway and will be reported in due course.

Acknowledgements

AKG and RB acknowledge CSIR, New Delhi, India for fellowships. SSG acknowledges DST, New Delhi (Grant No: SR/S1/PC-56/2008) for funding.

References

1 J. Hagen, *Industrial Catalysis: A practical Approach*, Wiley-VCH, 2006.
2 C. Mueller and D. Vogt, *Handbook of Green Chemistry: Green Catalysis*, 2009, **1**, 127–152.
3 M. Alvaro, C. Baleizao, D. Das, E. Carbonell and H. Garcia, *J. Catal.*, 2004, **228**, 254–258.
4 S. H. Cho, T. Gadzikwa, M. Afshari, S. T. Nguyen and J. T. Hupp, *Eur. J. Inorg. Chem.*, 2007, 4863–4867.
5 K. De Smet, S. Aerts, E. Ceulemans, I. F. J. Vankelecom and P. A. Jacobs, *Chem. Commun.*, 2001, 597–598.
6 D. Jayaprakash, Y. Kobayashi, S. Watanabe, T. Arai and H. Sasai, *Tetrahedron: Asymmetry*, 2003, **14**, 1587–1592.
7 A. Sakthivel, A. K. Hijazi, H. Y. Yeong, K. Kohler, O. Nuyken and F. E. Kuhn, *J. Mater. Chem.*, 2005, **15**, 4441–4445.
8 A. Sakthivel, S. Syukri, A. K. Hijazi and F. E. Kuhn, *Catal. Lett.*, 2006, **111**, 43–49.
9 T. J. Dickerson, N. N. Reed and K. D. Janda, *Chem. Rev.*, 2002, **102**, 3325–3344.
10 N. Madhavan, C. W. Jones and M. Weck, *Acc. Chem. Res.*, 2008, **41**, 1153–1165.
11 M. Pagliaro and R. Ciriminna, *J. Mater. Chem.*, 2005, **15**, 4981–4991.
12 D. Astruc, F. Lu and J. R. Aranzaes, *Angew. Chem., Int. Ed.*, 2005, **44**, 7852–7872.
13 A. Schatz, M. Hager and O. Reiser, *Adv. Funct. Mater.*, 2009, **19**, 2109–2115.
14 P. D. Stevens, G. Li, J. Fan, M. Yen and Y. Gao, *Chem. Commun.*, 2005, 4435–4437.
15 S. Tandukar and A. Sen, *J. Mol. Catal. A: Chem.*, 2007, **268**, 112–119.
16 S. Cousinie, M. Gressier, P. Alphonse and M. J. Menu, *Chem. Mater.*, 2007, **19**, 6492–6503.
17 A. Walcarius, M. Etienne and B. Lebeau, *Chem. Mater.*, 2003, **15**, 2161–2173.
18 D. J. Gorin, B. D. Sherry and F. D. Toste, *Chem. Rev.*, 2008, **108**, 3351–3378.
19 A. S. K. Hashmi, *Chem. Rev.*, 2007, **107**, 3180–3211.
20 A. S. K. Hashmi and M. Rudolph, *Chem. Soc. Rev.*, 2008, **37**, 1766–1775.
21 S. Carrettin, M. C. Blanco, A. Corma and A. S. K. Hashmi, *Adv. Synth. Catal.*, 2006, **348**, 1283–1288.
22 A. Corma, C. Gonzalez-Arellano, M. Iglesias, M. T. Navarro and F. Sanchez, *Chem. Commun.*, 2008, 6218–6220.
23 A. Corma, C. Gonzalez-Arellano, M. Iglesias, S. Perez-Ferreras and F. Sanchez, *Synlett*, 2007, 1771–1774.
24 C. Gonzalez-Arellano, A. Corma, M. Iglesias and F. Sanchez, *Eur. J. Inorg. Chem.*, 2008, 1107–1115.
25 L. Nebhcni and C. Barner-Kowollik, *Adv. Mater.*, 2009, **21**, 3442–3468.
26 V. V. Rostovtsev, L. G. Green, V. V. Fokin and K. B. Sharpless, *Angew. Chem., Int. Ed.*, 2002, **41**, 2596–2599.
27 A. S. K. Hashmi, J. P. Weyrauch, M. Rudolph and E. Kurpejovic, *Angew. Chem., Int. Ed.*, 2004, **43**, 6545–6547.
28 B. Malvi, B. R. Sarkar, D. Pati, R. Mathew, T. G. Ajithkumar and S. Sen Gupta, *J. Mater. Chem.*, 2009, **19**, 1409–1416.
29 C. Bartholome, E. Beyou, E. Bourgeat-Lami, P. Chaumont and N. Zydowicz, *Macromolecules*, 2003, **36**, 7946–7952.
30 D. A. Shirley, *Phys. Rev. B: Solid State*, 1972, **5**, 4709.
31 A. Dar, K. Moss, S. M. Cottrill, R. V. Parish, C. A. McAuliffe, R. G. Pritchard, B. Beagley and J. Sandbank, *J. Chem. Soc., Dalton Trans.*, 1992, 1907–1913.
32 J. Vicente, M. T. Chicote and M. D. Bermudez, *J. Organomet. Chem.*, 1984, **268**, 191–195.
33 S. Singh and B. L. V. Prasad, *J. Phys. Chem. C*, 2007, **111**, 14348–14352.
34 Y. Chen, W. Yan, N. G. Akhmedov and X. Shi, *Org. Lett.*, 2010, **12**, 344–347.

